

High-Throughput Screening of an FDA-Approved Drug Library Identifies Inhibitors against Arenaviruses and SARS-CoV-2

Weiwei Wan, Shenglin Zhu, Shufen Li, Weijuan Shang, Ruxue Zhang, Hao Li, Wei Liu, Gengfu Xiao,* Ke Peng,* and Leike Zhang*

Cite This: <https://dx.doi.org/10.1021/acsinfectdis.0c00486>

Read Online

ACCESS |

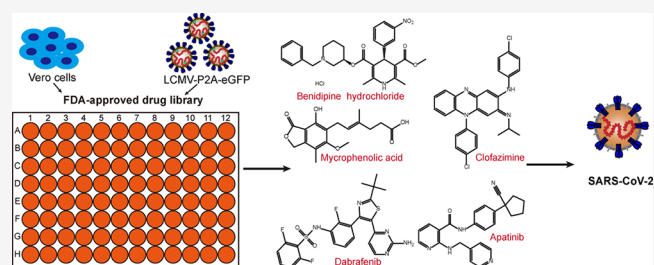
Metrics & More

Article Recommendations

Supporting Information

ABSTRACT: Arenaviruses are a large family of enveloped negative-strand RNA viruses that include several causative agents of severe hemorrhagic fevers. Currently, there are no FDA-licensed drugs to treat arenavirus infection except for the off-labeled use of ribavirin. Here, we performed antiviral drug screening against the Old World arenavirus lymphocytic choriomeningitis virus (LCMV) using an FDA-approved drug library. Five drug candidates were identified, including mycophenolic acid, benidipine hydrochloride, clofazimine, dabrafenib, and apatinib, for having strong anti-LCMV effects. Further analysis indicated that benidipine hydrochloride inhibited LCMV membrane fusion, and an adaptive mutation on the LCMV glycoprotein D414 site was found to antagonize the anti-LCMV activity of benidipine hydrochloride. Mycophenolic acid inhibited LCMV replication by depleting GTP production. We also found mycophenolic acid, clofazimine, dabrafenib, and apatinib can inhibit the newly emerged severe acute respiratory syndrome coronavirus 2 (SARS-CoV-2) infection. Owing to their FDA-approved status, these drug candidates can potentially be used rapidly in the clinical treatment of arenavirus and SARS-CoV-2 infection.

KEYWORDS: drug screening, arenavirus, SARS-CoV-2, benidipine hydrochloride, mycophenolic acid



Arenaviruses are enveloped viruses with bisegmented, negative-stranded RNA genomes comprising a large (L) and a small (S) segment. Both RNA segments use an ambisense coding strategy to encode two open reading frames (ORFs) in opposite orientations, and they are separated by a stable hairpin structure called the intergenic region (IGR), which mediates the transcription termination.^{1,2} The L segment encodes the RNA-dependent RNA polymerase L protein and zinc finger matrix protein Z, whereas the S segment encodes the nucleoprotein (NP) and the envelope glycoprotein complex (GPC).^{3,4} GPC is post-translationally processed by the signal peptidase and the SKI-1/S1P cellular proteases to produce the mature surface virion glycoproteins GP1 and GP2.^{5,6} GPC also has a cotranslationally processed stable signal peptide (SSP) with a transmembrane hairpin structure, and its ectodomain loop triggers membrane fusion.^{7–9} These three polypeptides form the mature GP1/GP2/SSP complex present at the surface of mature virions, while they also mediate receptor recognition and cell entry.^{10,11}

The family *Arenaviridae* can be divided into two genera: *Mammarenavirus* and *Reptarenavirus*.¹² *Mammarenavirus* members are classified into two groups, mainly based on antigenic properties and geographical distribution: Old World (OW) and New World (NW) arenaviruses.² The OW arenaviruses include Lassa virus (LASV) and lymphocytic choriomeningitis virus (LCMV), whereas the NW arenaviruses include Junin

virus (JUNV) and Machupo virus (MACV). While *mammarenaviruses* generally cause chronic and asymptomatic infections in their natural host rodents, several arenaviruses such as LASV, JUNV, and MACV can cause severe hemorrhagic fever in infected humans, posing serious threats to public health.^{13,14} It was reported that 100 000–300 000 LASV infections occur in West Africa annually, with an estimated 1–2% mortality rate.¹⁵ The case fatality rate of Argentine hemorrhagic fever caused by JUNV infection without treatment is between 15% and 30%.¹⁶

LCMV is also a neglected human pathogen with clinical significance carried by its natural host, *Mus musculus* and other rodents worldwide.^{17–19} In immunocompetent individuals, LCMV usually causes asymptomatic or mild infection with flu-like symptoms; however, severe cases have central nervous system clinical manifestations, including aseptic meningitis, meningoencephalitis, abortion, hydrocephalus, and chorioretinitis.^{20,21} Moreover, the virus is fatal to people with immune deficiency, especially organ transplantation patients.^{22,23} In

Special Issue: Gut Pathogens

Received: July 9, 2020

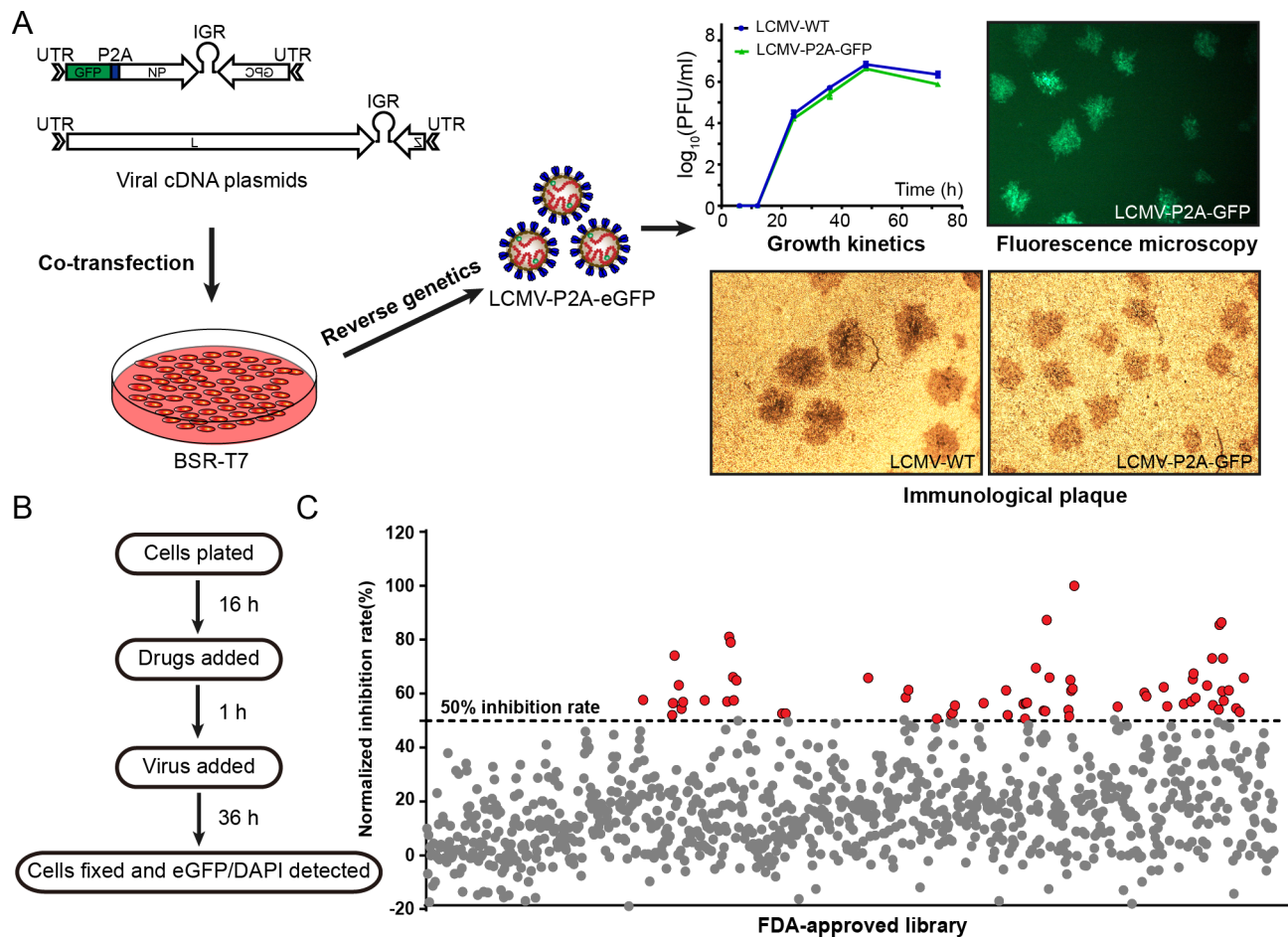


Figure 1. Cell-based high-throughput screening (HTS) using LCMV-P2A-eGFP to identify inhibitors of LCMV replication. (A) Construction of the eGFP-expressed recombinant virus LCMV-P2A-eGFP. Self-splicing sequence P2A and eGFP were inserted between NP and UTR to get the recombinant virus LCMV-P2A-eGFP. Vero cells were infected with LCMV and LCMV-P2A-eGFP (MOI = 0.1). At 6, 12, 24, 36, 48, and 72 h postinfection, the supernatant was collected, and viral titers were tested and growth curves of the two viruses were generated. Viral plaque was observed using an immunological plaque assay and a fluorescence microscope. (B) Flowchart of cell-based HTS using LCMV-P2A-eGFP to identify inhibitors of LCMV replication. (C) HTS for primary candidates of inhibiting LCMV infection from a 1018 FDA-approved drugs library. Inhibition ratios of all drugs from the primary screen were represented by scattered points. The red color points indicated the 63 drugs with inhibition rates $\geq 50\%$ that were selected for the secondary screening.

addition, LCMV can be vertically transmitted from infected pregnant women to their fetus, which would cause congenital LCMV infection of the infant, resulting in severe damage to the brain and eyes.^{24,25} The lack of FDA-approved vaccines or specific drugs limited the options to treat arenavirus infection, besides the off-label use of ribavirin.^{26–29} Thus, there is an urgent need for an innovative and effective therapeutic approach to mitigate arenavirus infections.

The coronavirus disease 2019 (COVID-19) caused by the novel severe acute respiratory syndrome coronavirus 2 (SARS-CoV-2) has now spread to more than 200 countries, posing a global public health concern. As of 23 October 2020, over 41 million COVID-19 cases and over 1.1 million deaths have been reported, globally.³⁰ The development of effective antiviral drugs to treat COVID-19 patients is of great urgency. Screening FDA-approved drugs for antiviral compounds provides a promising potential for repurposed drug application, as the clinical safety of the identified drug candidate was already extensively evaluated. Here, by screening an FDA-approved drug library, we found that mycophenolic acid, benidipine hydrochloride, clofazimine, dabrafenib, and apatinib can inhibit LCMV and SARS-CoV-2 infection in vitro. These

drugs have the potential to be used rapidly in the clinical treatment of arenavirus and SARS-CoV-2.

RESULTS

Screening of the FDA-Approved Drug Library to Identify Compounds with Anti-LCMV Activity. To screen the anti-LCMV drugs, recombinant virus LCMV-P2A-eGFP, which expresses eGFP as an indicator for LCMV replication, was used for large-scale screening analysis for anti-LCMV drugs.³¹ No significant changes in the growth curves were observed between LCMV-P2A-eGFP and wild-type LCMV (Figure 1A). A library containing 1018 FDA-approved drugs (Selleck) was employed to screen the anti-LCMV drugs. For the primary screen, Vero cells preseeded in 96-well plates were treated with 10 μM of the drugs and then infected with LCMV-P2A-eGFP at a multiplicity of infection (MOI) of 0.1. At 36 h postinfection (p.i.), cells were fixed and its eGFP intensity was detected using the high content imaging system (Figure 1B). The percentage of infected cells in each well was calculated through automated imaging and quantitative analysis. The statistical reliability was determined by calculating the Z' factor, as previously described,³² a Z' factor

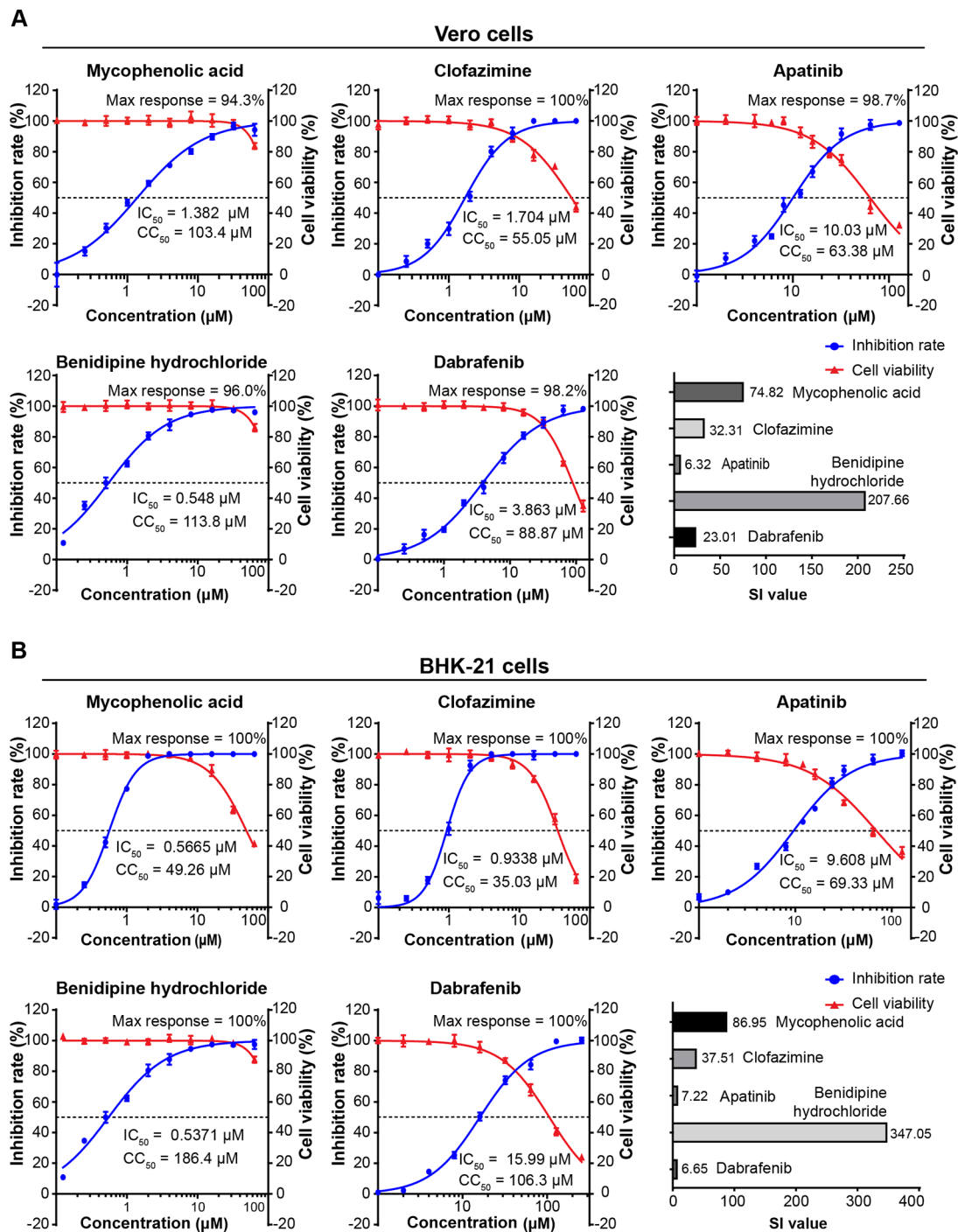


Figure 2. Dose-dependent effects of mycophenolic acid, clofazimine, apatinib, benidipine hydrochloride, and dabrafenib on LCMV replication in Vero and BHK-21 cells. (A) Dose-dependent effects of mycophenolic acid, clofazimine, apatinib, benidipine hydrochloride, and dabrafenib on LCMV replication in Vero cells. A series of concentrations of indicated drugs or DMSO pretreated Vero cells were infected with LCMV (MOI = 0.1). At 36 h p.i., total RNA was extracted and intracellular viral RNA level was detected by qRT-PCR, and cell viability was detected by MTT assay. The inhibition rate and cell viability were normalized by the value of the DMSO-treated cells. The IC_{50} and CC_{50} values were calculated using Graphpad Prism 6 software. (B) Dose-dependent effects of mycophenolic acid, clofazimine, apatinib, benidipine hydrochloride, and dabrafenib on LCMV replication in BHK-21 cells.

of 0.65 in our experiment indicated that the primary screening was reliable. Ribavirin was also used as a positive control for this screening, and the viral inhibition rate and cell cytotoxicity of ribavirin were calculated (Figure S1A). To this end, 63 drugs were selected for secondary screening based on >50% viral inhibition rate and <50% cell cytotoxicity (Figure 1C).

Of these 63 drugs, five drugs (mycophenolic acid, clofazimine, apatinib, benidipine hydrochloride, and dabrafenib) have been shown to inhibit LCMV replication in a dose-dependent manner. The half maximal inhibitory concentration (IC_{50}) and half maximal cytotoxic concentration (CC_{50}) values of these drugs were determined using Vero and BHK-21 cells, respectively. Briefly, cells were pretreated at indicated

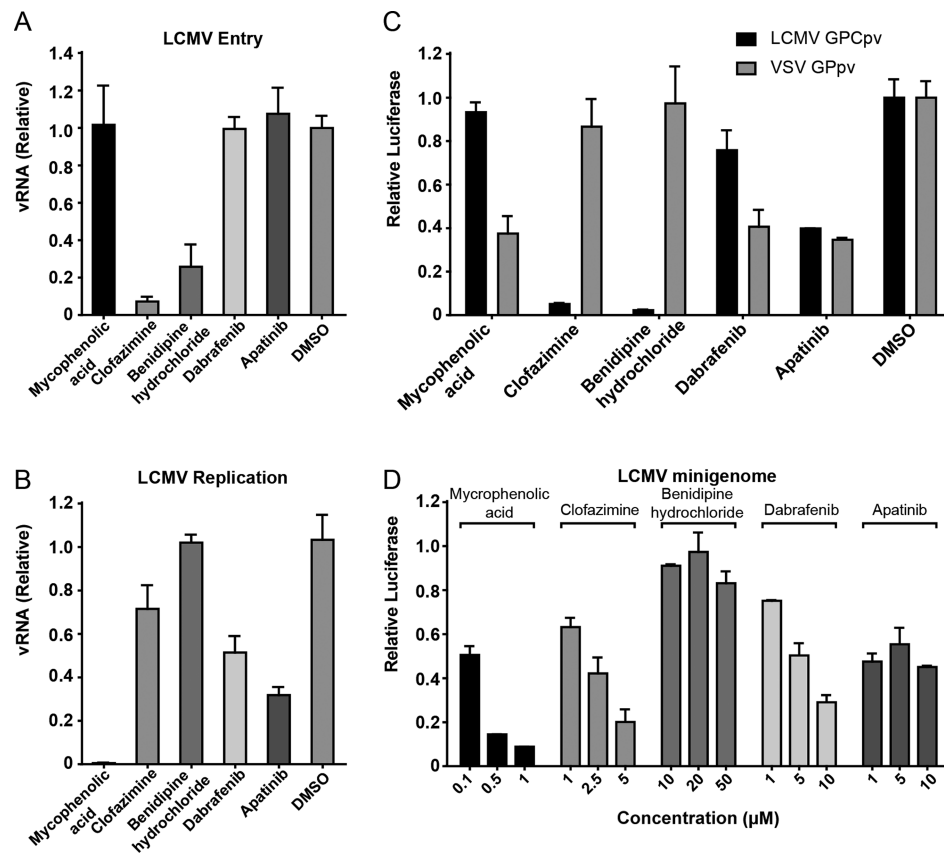


Figure 3. The effects of mycophenolic acid, clofazimine, apatinib, benidipine hydrochloride, and dabrafenib on the life cycle stages of LCMV. (A) The effects of indicated drugs on viral entry stage. The drugs were added 1 h preinfection, and at 3 h p.i., cells were washed and fresh medium was added to remove the uninfected virus and drugs. The cells were lysed and viral RNA level was detected by qRT-PCR at 16 h p.i. (B) The effects of indicated drugs on viral replication stage. These drugs were added 3 h p.i. and preserved until the cells were collected. The cells were lysed and viral RNA level was detected at 16 h p.i. (C) The effects of these drugs on LCMV GPC-coated pseudotype VSV. The drug- or DMSO-treated cells were infected with LCMV GPC- and VSV G-coated pseudotype VSV. At 24 h p.i., the replication level of pseudotype VSV was measured. (D) The effects of these drugs on viral minigenome activity. BSR-T7 cells were transfected with LCMV MG plasmids, and then treated with indicated drugs or DMSO. The luciferase activity (representing MG activity) was acquired at 36 h post-transfection.

concentrations of mycophenolic acid, clofazimine, apatinib, benidipine hydrochloride, and dabrafenib for 1 h prior to LCMV infection at MOI of 0.1. Next, the cells were collected, and the virus RNA level was analyzed by quantitative Real-time PCR (qRT-PCR) at 36 h p.i. to calculate the inhibition ratio. Furthermore, cell viability was measured using the MTT assay. The IC_{50} , CC_{50} , and selectivity index (SI) values of these five drugs on Vero and BHK-21 cells were calculated (Figure 2A,B), with benidipine hydrochloride and mycophenolic acid exhibiting strong antiviral activity with low cytotoxicity (SIs > 50) in both Vero and BHK-21 cells. We also tested all these compounds in A549 and primary mouse spleen cells, and found mycophenolic acid, clofazimine, benidipine hydrochloride, and dabrafenib can inhibit LCMV replication, while apatinib showed low anti-LCMV activity (Figure S2 and S3).

The Selected Drugs Inhibited Different Viral Life-Cycle Stages. Our preliminary data indicated that LCMV initiated its genome replication but not budding in the BHK-21 cells at 16 h p.i. To dissect the stages of the viral life-cycle at which these drugs are implicated, BHK-21 cells were pretreated with each of the five drugs for 1 h prior to LCMV infection to 3 h p.i. and also post-treated with these 5 drugs from 3 to 16 h p.i. to represent the virus entry and replication stages, respectively. At the end of 16 h p.i., the cells were lysed, and the relative virus RNA level was analyzed by

qRT-PCR. As shown in Figure 3A and 3B, clofazimine and benidipine hydrochloride exert an antiviral effect during the entry phase, suggesting that clofazimine and benidipine hydrochloride may inhibit the viral entry stage of LCMV. In contrast, mycophenolic acid, apatinib, and dabrafenib could inhibit LCMV replication. Interestingly, LCMV replication was slightly repressed in clofazimine-treated cells, suggesting that clofazimine might inhibit both the entry and the replication stages of the life cycle.

We also employed the LCMV GPC-coated pseudotype vesicular stomatitis virus (VSV) to test the effects of these five drugs on LCMV GPC-mediated virus entry. The VSV G-coated pseudotype VSV was used as a control virus to exclude the effect of these drugs on VSV genome replication. The drugs or DMSO was added to the BHK-21 cells 1 h preinfection; then, the cells were infected with LCMV GPC- or VSV G-coated pseudotype VSV. At 24 h p.i., the cells were lysed, and the luciferase activity was measured. We found that LCMV GPC-coated pseudotype VSV could be inhibited by clofazimine, benidipine hydrochloride, and apatinib, of which apatinib also disturbed the VSV G-coated pseudotype VSV replication (Figure 3C), suggesting that clofazimine and benidipine hydrochloride could inhibit LCMV GPC-mediated virus entry.

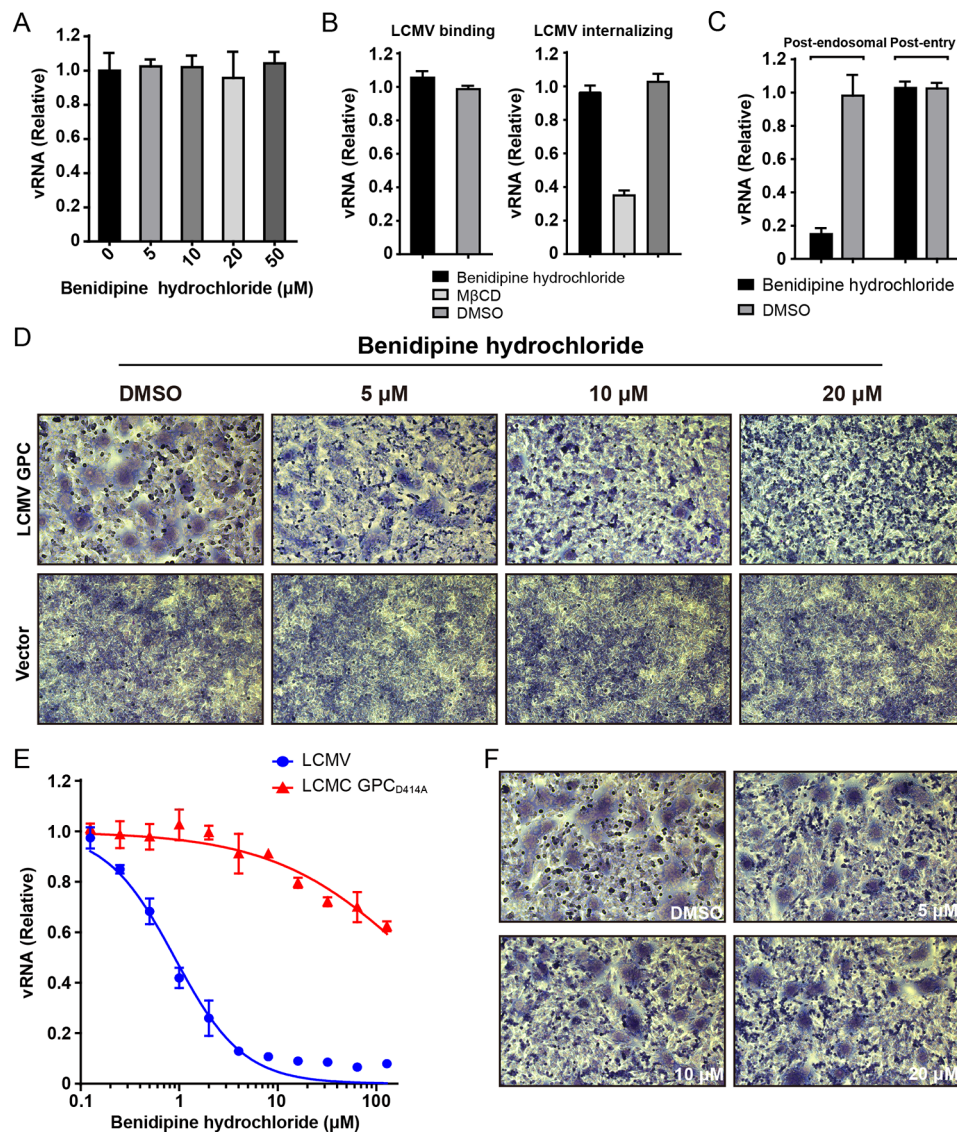


Figure 4. The effect of Benidipine hydrochloride on the entry stages of LCMV. (A) The virucidal effect of benidipine hydrochloride on LCMV virions. Virus was incubated with different concentrations of benidipine hydrochloride or the vehicle for 1 h. Then, the virus was diluted 1000-fold and added to the BHK-21 cells. At 24 h p.i., cells were lysed and viral RNA was tested by qRT-PCR. (B) The effect of benidipine hydrochloride on binding and internalization of LCMV. (C) The effect of benidipine hydrochloride on the postendosomal step of LCMV. (D) Effect of benidipine hydrochloride on LCMV GPC-mediated pH-dependent membrane fusion. BHK-21 cells were transfected with pCAGGS-GPC and vector, and 24 h later, cells were treated with benidipine hydrochloride or vehicle, then treated with acidized medium (pH of 5.0). After 20 min, cells were treated with normal culture medium, and membrane fusion could be observed within 30 min. The cells were fixed with methanol and stained with Giemsa. (E) The dose-dependent effect of benidipine hydrochloride on the LCMV GPC-D414A. Different concentrations of benidipine hydrochloride treated BHK-21 cells were infected with the LCMV GPC-D414A and wild-type LCMV. At 36 h p.i., cells were lysed and viral RNA was tested by qRT-PCR. (F) The effect of benidipine hydrochloride on the D414 mutant GPC-mediated pH-dependent membrane fusion. The BHK-21 cells were transfected with pCAGGS-GPC-D414A. At 24 h post-transfection, the LCMV GPC-mediated pH-dependent membrane fusion was monitored.

To further explore whether these drugs inhibit LCMV genome replication and transcription, the LCMV minigenome (MG) rescue system was employed. The BSR-T7 cells were treated with different concentrations of drugs 4 h post-MG plasmid transfection. The cells were lysed, and the luciferase activity was tested 36 h post-transfection. As shown in Figure 3D, the MG activities could be inhibited by mycophenolic acid, apatinib, dabrafenib, and clofazimine, but not by benidipine hydrochloride, suggesting that mycophenolic acid, apatinib, dabrafenib, and clofazimine could inhibit LCMV genome replication or transcription, which was consistent with the above results (Figure 3A,B).

Benidipine Hydrochloride Inhibits LCMV pH-Dependent Membrane Fusion. Since benidipine hydrochloride showed the strongest anti-LCMV efficacy among these five drugs (SI > 200), the antiviral mechanism of benidipine hydrochloride was explored. The above data indicated that benidipine hydrochloride could inhibit LCMV infection at the virus entry step. After binding to the receptor on the cell surface, the arenavirus was internalized to the endosome, and then membrane fusion occurred at a low pH.^{33,34}

We first examined whether benidipine hydrochloride irreversibly bound to LCMV and caused the loss of virus infectivity. We incubated LCMV with different concentrations

of benidipine hydrochloride up to 50 μM or DMSO for 1 h at 37 °C. Then, the drug-treated virus was diluted 1000-fold to exclude the effect of any residual drug. The diluted virus was added to the BHK-21 cells and incubated for 24 h, then the virus RNA level was detected by qRT-PCR. However, no significant difference was observed between benidipine hydrochloride and vehicle, indicating that benidipine hydrochloride did not have virucidal effects on LCMV (Figure 4A).

Next, two experiments were performed to determine whether benidipine hydrochloride affects LCMV binding or internalization. First, to identify the effect of benidipine hydrochloride on LCMV binding, benidipine hydrochloride pretreated BHK-21 cells were precooled at 4 °C for 15 min, then infected with precooled LCMV (MOI = 0.1). After incubated at 4 °C for 1 h and washed three times with cold PBS, cells were lysed and bound viral RNA was measured by qRT-PCR. Second, to identify the effect of benidipine hydrochloride on LCMV internalization, benidipine hydrochloride-treated cells were infected with LCMV (MOI = 0.1) and incubated at 37 °C for 3 h. Then, the supernatant was removed and cells were digested with trypsin to remove bound virion. Internalized viral RNA was also measured by qRT-PCR. As shown in Figure 4B, the RNA level of bound or internalized viral load did not change significantly, suggesting that benidipine hydrochloride did not inhibit virus binding or internalization.

As benidipine hydrochloride may affect the later stages of LCMV entry, a postendosomal assay developed previously by Banerjee et al. and Oppliger et al. was employed to identify the antiviral target of benidipine hydrochloride.^{34,35} BHK-21 cells were treated with ammonium chloride and infected with LCMV (MOI = 0.1) to avoid membrane fusion and synchronize the virus in the endosome. At 1 h p.i., benidipine hydrochloride was added to cells and incubated for 30 min, then the supernatant was removed and the fresh medium containing benidipine hydrochloride was added to permit virus membrane fusion. At 16 h p.i., viral RNA level was measured by qRT-PCR. To exclude the potential effects of benidipine hydrochloride on virus replication during the postendosomal assay, a supplementary postentry assay was developed. BHK-21 cells were infected with LCMV (MOI = 0.1). At 1 h p.i., benidipine hydrochloride was added to cells and incubated for 16 h then tested by qRT-PCR. As shown in Figure 4C, benidipine hydrochloride treatment could significantly decrease LCMV infection at the postendosomal stage and the target phase was identified after virus exposure to the low-pH environment in the endosome.

After binding to the receptor, arenavirus entered the target cell via endocytosis and was delivered to the late endosome, where low-pH-dependent membrane fusion occurred.³⁴ To identify whether benidipine hydrochloride affected GPC-mediated membrane fusion, a series of concentrations of benidipine hydrochloride were treated on an LCMV GPC-transfected cell fusion model. The BHK-21 cells were transfected with pCAGGS-GPC 24 h prior. Then, the cells were treated with benidipine hydrochloride or the vehicle and exposed to a pH 5.0 medium for 20 min. Membrane fusion could be observed in 30 min, with the presence of benidipine hydrochloride throughout the entire process of this experiment. In the DMSO-treated LCMV GPC-transfected cells, obvious membrane fusion was observed in comparison to the vector-transfected control or the cells without acidification. Furthermore, benidipine hydrochloride strongly decreased cell

fusion as the concentration increased (Figure 4D). This suggested that benidipine hydrochloride could strongly prevent LCMV GPC-mediated membrane fusion.

LCMV with GPC D414A Mutation Is Resistant to Benidipine Hydrochloride Treatment. After serial passages in the presence of benidipine hydrochloride, a drug-resistant LCMV was obtained. Via sequence analysis of the genome of the resistant LCMV, a 414th amino acid aspartic acid (D) to alanine (A) mutation on GPC was found, namely, GPC-D414A. Then, LCMV GPC-D414A was rescued, no significant changes in the growth curves and pH of fusion were observed between wild type and mutant LCMV (Figure S5), while the inhibition efficacy of benidipine hydrochloride treatment on LCMV GPC-D414A was significantly lower than that of wild type LCMV (Figure 4E, Figure S5B), suggesting that the GPC D414 site is important to the antiviral efficacy of benidipine hydrochloride.

As mentioned above, low-pH treatment of the LCMV GPC-transfected cells could cause cell membrane fusion, which could be inhibited by benidipine hydrochloride. Thus, we also explored the effect of benidipine hydrochloride on D414A mutant LCMV GPC-mediated membrane fusion. As shown in Figure 4F, the cell membrane fusion of the D414A mutant LCMV GPC-transfected cells could not be affected by benidipine hydrochloride treatment, while the wild type was significantly inhibited. These results suggested that benidipine hydrochloride might target LCMV GPC D414 site to prevent GPC-mediated membrane fusion.

Effect of Benidipine Hydrochloride on Hemorrhagic Fever Arenavirus GPC-Coated Pseudotype VSV. To verify that benidipine hydrochloride could also inhibit the entry step of other hemorrhagic fever arenaviruses, we tested the antiviral effect of benidipine hydrochloride on some other arenavirus GPC-coated pseudotype VSV. The VSV G-coated pseudotype VSV was used to exclude the side effects of benidipine hydrochloride on VSV replication. As shown in Figure 5A, benidipine hydrochloride could significantly inhibit LASV, JUNV, and MACV GPC-coated pseudotype VSV but not VSV G-coated pseudotype VSV, demonstrating that benidipine hydrochloride had broad-spectrum antiarenavirus effects. The IC₅₀ values of benidipine hydrochloride on these arenavirus GPC-coated pseudotype VSV were 1 μM , which is comparable with the effect on LCMV. The antiviral effect of benidipine hydrochloride on recombinant LCMV expressing LASV GPC was also tested (Figure S4B).

Other Dihydropyridines Could Also Inhibit LCMV Infection. Benidipine hydrochloride is a member of the dihydropyridine (DHP)-derived calcium channel blockers (CCBs).³⁶ CCBs are usually used in the clinical treatment of hypertension and vessel stiffness.^{37,38} Thus, we selected some other DHP-derived CCBs to examine their anti-LCMV effect. The results showed that cilnidipine, amlodipine, felodipine, nicardipine, clevidipine, and nilvadipine all had a dose-dependent inhibition effect on LCMV infection (Figure 5B). As the CCBs could significantly inhibit LCMV, we surmised that whether the antiviral effect of benidipine hydrochloride was associated with the inhibition of calcium fluxes. The antiviral effects of calcium chelator BAPTA were determined, and the results showed that BAPTA did not affect LCMV multiplication (Figure S6A). We also found that the treatment of calcium free medium, which could affect SFTSV replication by preventing calcium flux,³⁹ could not affect LCMV replication here (Figure S6B), suggesting that the effect of

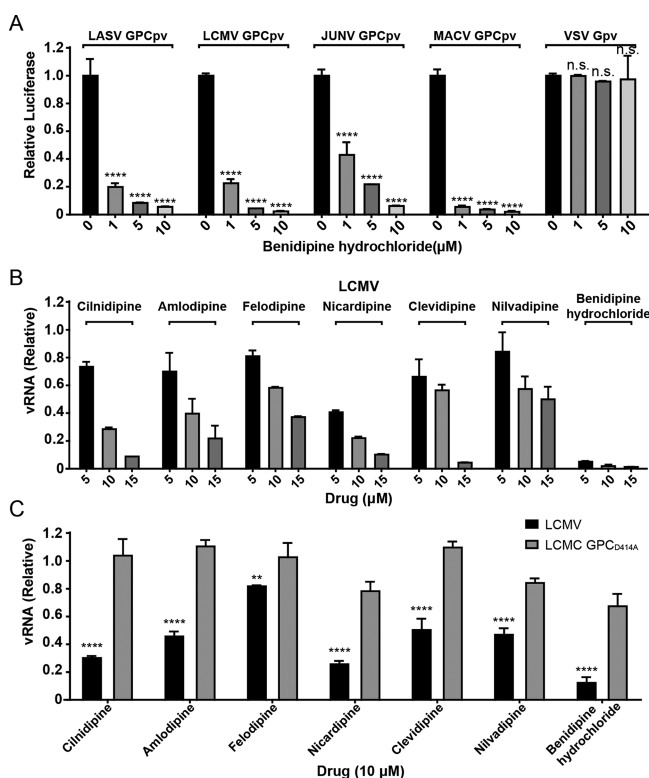


Figure 5. The effect of benidipine hydrochloride on other arenaviruses and analogous antiviral effects of other DHPs. (A) Antiviral effect of benidipine hydrochloride on other arenaviruses. BHK-21 cells were pretreated with 1 μM , 5 μM , or 10 μM benidipine hydrochloride or DMSO, and then infected with LASV GPC, LCMV GPC, JUNV GPC, MACV GPC, and VSV G-coated pseudotype VSV. At 24 h p.i., cells were lysed and viral replication activity was detected to calculate the inhibition effect of benidipine hydrochloride. Comparison of mean values between benidipine hydrochloride-treated group and DMSO group was analyzed by Student's *t* test. **P* < 0.05; ***P* < 0.01; ****P* < 0.001; *****P* < 0.0001. (B) The effect of the other DHPs on LCMV replication. Cilnidipine, amlodipine, felodipine, nicardipine, clevidipine, nilvadipine, benidipine hydrochloride, or vehicle pretreated BHK-21 cells were infected with LCMV (MOI = 0.1). Cells were lysed and viral RNA was tested by qRT-PCR at 36 h p.i. (C) The antiviral effect of the other DHPs on the LCMV GPC-D414A.

benidipine HCl on LCMV entry is not related to calcium flux. The antiviral effect of these DHPs was also tested on the mutant LCMV GPC-D414A. Compared to wild-type LCMV, the mutant virus showed more resistibility to these DHPs (Figure 5C). Thus, we concluded that the drug resistance of the LCMV GPC-D414A mutant was of a broad-spectrum nature with respect to DHPs, suggesting that they might share a common antiviral mechanism.

Mycophenolic Acid, Apatinib, Dabrafenib, and Clofazimine Can Inhibit the Replication of SARS-CoV-2. As mycophenolic acid, apatinib, dabrafenib and clofazimine can inhibit the replication of LCMV, we then explored whether these drugs could affect the infection of SARS-CoV-2. Vero E6 cells were pretreated with a series of concentrations of mycophenolic acid, clofazimine, apatinib, and dabrafenib, and then infected with SARS-CoV-2 at an MOI of 0.01. Remdesivir was used as a positive control (Figure S1B). Viral genome RNA was extracted from the supernatant collected at 24 h p.i., and the antiviral efficacies of these drugs were calculated by

quantification of the viral copy numbers detected via qRT-PCR analysis. Cell cytotoxicities under the same conditions were also evaluated by MTT assay. Among these drugs, a low concentration of mycophenolic acid (IC_{50} = 0.101 μM , CC_{50} > 100 μM) and clofazimine (IC_{50} = 0.562 μM , CC_{50} = 100.6 μM) could strongly inhibit SARS-CoV-2 replication in vitro; dabrafenib (IC_{50} = 2.264 μM , CC_{50} > 100 μM) and apatinib (IC_{50} = 15.63 μM , CC_{50} > 100 μM) also have antiviral efficacy on SARS-CoV-2. The anti-SARS-CoV-2 activity of these drugs was also determined by detecting the intracellular level of NP using immunofluorescence assay (Figure 6A).

Extra Addition of Guanosine Could Reverse the Antiviral Efficacy of Mycophenolic Acid. Among these four drugs, mycophenolic acid showed the strongest anti-SARS-CoV-2 efficacy (SI > 1000). Mycophenolic acid is an inhibitor of cellular enzyme inosine monophosphate dehydrogenase (IMPDH), which is important for guanosine synthesis. The inhibition of IMPDH by mycophenolic acid could cause cellular GTP depletion, which is essential for virus replication.⁴⁰ Mycophenolic acid has been reported to inhibit multiple viruses including dengue virus, coxsackie B3 virus, hepatitis C virus, hepatitis E virus.^{41–44} As shown in Figure 6B, mycophenolic acid could inhibit LCMV infection, but the inhibition efficacy was significantly reduced after the exogenous addition of guanosine, which can restore the intracellular GTP level. We also found that mycophenolic acid could inhibit SARS-CoV-2 replication significantly, and this inhibition was also reduced upon the addition of guanosine. These results indicated that mycophenolic acid inhibits arenavirus LCMV and coronavirus SARS-CoV-2 infection by inhibiting IMPDH activity and depleting intracellular GTP, and this inhibition can be rescued by extra addition of guanosine.

DISCUSSION

Benidipine hydrochloride is a long-acting dihydropyridine-derived CCB for the treatment of hypertension and angina pectoris,³⁷ and it blocks triple L-, N-, and T-type calcium channels.⁴⁵ The efficiency of benidipine hydrochloride is strong and long-lasting due to its higher binding capacity to the DHP binding site on the voltage-gated calcium channel (VGCC) and the plasma membrane compared to other CCBs.^{46–49} In addition to the antihypertensive effects, benidipine hydrochloride also shows renoprotective effects,^{50,51} vascular endothelial protective effects,³⁸ and cardioprotective effects.⁵² The toxicity of benidipine hydrochloride was assessed in mice, rats, guinea pigs, rabbits, and dogs, and only mild and reversible side effects were observed, whereas serious problems including carcinogenicity, antigenicity, or teratogenicity did not occur.⁵³ Moreover, a clinical study further indicated that benidipine hydrochloride causes fewer side effects than other CCBs.^{45,54} This demonstrates that benidipine hydrochloride is a safe drug for clinical use.

In this study, benidipine hydrochloride was demonstrated to have a strong antiviral effect on LCMV in different cell lines with IC_{50} values lower than 1 μM . We also found that benidipine hydrochloride can effectively inhibit LCMV replication in primary mouse spleen cells; however, the effect of benidipine hydrochloride on LCMV in vivo still needs further investigation. The different time-of-addition experiments revealed that the main target of benidipine hydrochloride is the early process of the LCMV life cycle. The arenavirus GPC-coated pseudotype VSV, which was con-

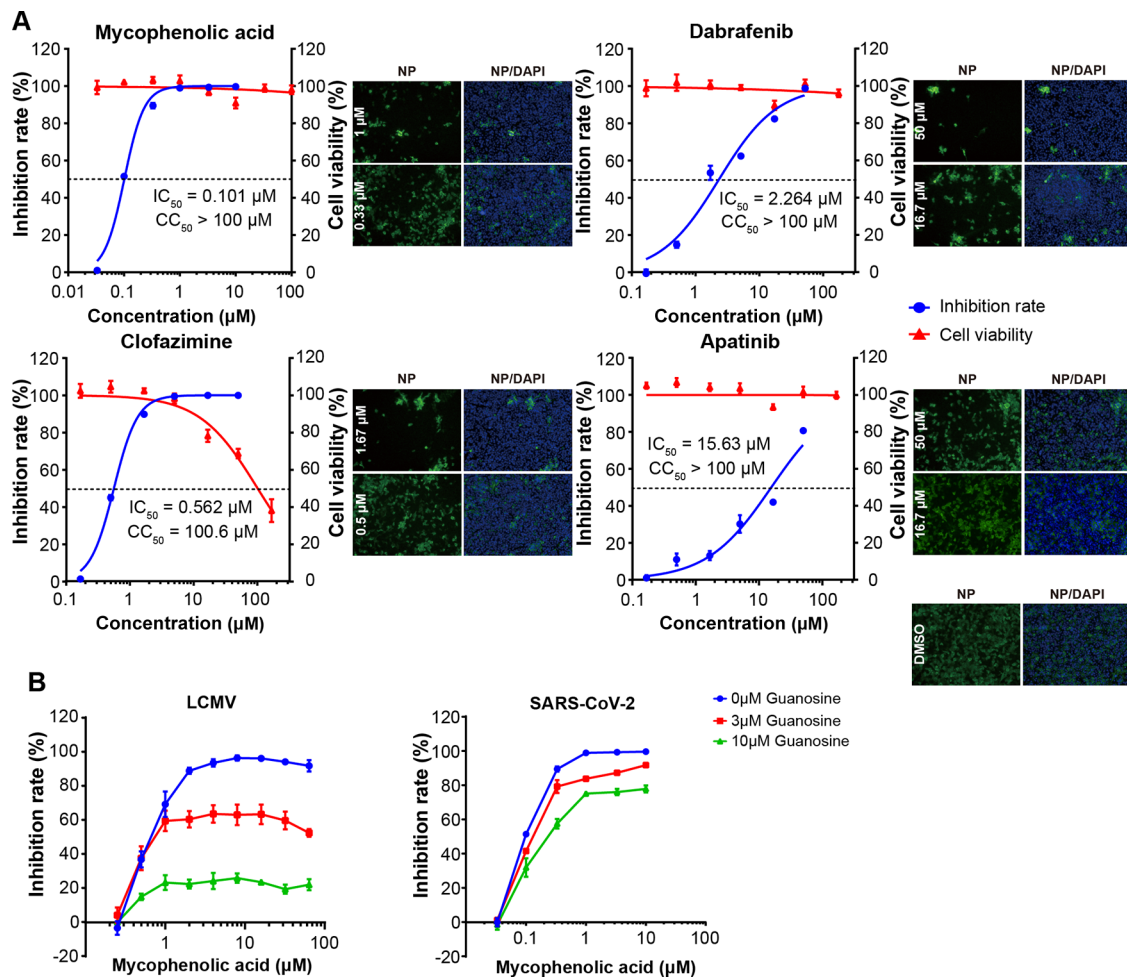


Figure 6. Dose-dependent effects of mycophenolic acid, apatinib, dabrafenib, and clofazimine on SARS-CoV-2 replication in Vero E6 cells. (A) Determination of indicated drugs IC_{50} and CC_{50} values of SARS-CoV-2 on Vero E6 cells. A series of concentrations of drugs or DMSO pretreated Vero E6 cells were infected with SARS-CoV-2 (MOI = 0.01). At 24 h p.i., the supernatant was collected, and viral RNA was extracted and detected by qRT-PCR. Cell viability was detected by MTT assay. The inhibition rate and cell viability were normalized by the value of the DMSO-treated cells. The IC_{50} and CC_{50} values were calculated by Graphpad Prism 6 software. Cells were fixed and probed with the primary antibody against viral nucleocapsid protein of a bat SARS-related coronavirus. (B) Reversion of the antiviral effect of mycophenolic acid by the extra addition of guanosine. Vero or Vero E6 cells were treated by a series of concentrations of mycophenolic acid and extra guanosine, and then infected with LCMV (MOI = 0.1) or SARS-CoV-2 (MOI = 0.01). At 24 h p.i., the supernatant of SARS-CoV-2 infected Vero E6 cells was collected. Viral RNA in the supernatant was extracted and measured with qRT-PCR. At 36 h p.i., total RNA of LCMV infected cells was extracted, and the relative intracellular viral RNA level was determined by qRT-PCR.

structed to mimic the arenavirus entry process, was also strongly inhibited by benidipine hydrochloride treatment, while the wild-type VSV was not affected. This provided further proof that benidipine hydrochloride targets the entry step of arenavirus infection. OW arenaviruses LASV and LCMV utilize α -dystroglycan,^{55,56} while NW arenaviruses JUNV and MACV use transferrin receptor 1 as their cellular receptors.⁵⁷ VSV G is a class III fusion active protein with different fusion mechanisms to arenavirus GPs.⁵⁸ However, both VSV and arenavirus go through a pH-dependent membrane fusion process to transport viral replication material into the cytoplasm. This suggests that benidipine hydrochloride does not affect virus entry by changing the endosomal pH; it may bind to specific sites on the arenavirus GP or affect the specific fusion process of arenavirus.

To investigate whether benidipine hydrochloride has an irreversible binding affinity to the GPC displayed on viral particles, we incubated high-titer LCMV with benidipine hydrochloride prior to infection to carry out the virucidal

experiment, and LCMV infection was not blocked. In previous reports, the K33 residue on the SSP was shown to play an important role in pH sensing and triggering following membrane fusion.⁸ The D414 residue was identified to interact with the K33 residue on SSP to mediate the activation of membrane fusion, and it could complement K33 mutation-induced fusion deficiency.⁵⁹ The D414 residue is also sensitive to inhibitors that bind at the SSP–GP2 interface and prevent low-pH-induced membrane fusion.^{60–62} In our study, the D414 mutation on LCMV GPC could offset the antiviral effect of benidipine hydrochloride and other DHPs. We propose that benidipine hydrochloride might reversibly bind to the D414 residue, or the binding might only occur at low pH. This binding might hinder the SSP–GP2 interaction; the pH sensing and membrane fusion triggering ability of SSP–GP2 is interrupted, and as a consequence, virus proliferation is prevented.

There are also other VGCC blockers, including nifedipine, verapamil, gabapentin, lacidipine, and tetrandrine, that could

inhibit virus infection by interfering with the virus entry stage.^{63–65} Knockdown of VGCC subunits or treatment with channel blockers diminished JUNV-cell fusion and entry into cells and thereby decreased infection.⁶³ And a recent study indicated that VGCC is critical for cellular binding and entry of the NW arenaviruses JUNV and Tacaribe virus, suggesting that zoonotic viruses could spread via this receptor.⁶⁶ Filovirus, including Ebola virus and Marburg virus, entry could be inhibited by L-type calcium blocker verapamil.⁶⁷ Influenza A virus binding to the host cell surface is mediated by the attachment of virus hemagglutinin to sialylated VGCC, and its entry could be inhibited by CCB or VGCC knock-down.⁶⁸ Other calcium channels, two-pore channels (TPCs), are also required for Ebola virus entry.⁶⁹

Hemorrhagic fever causes severe public health problems in humans;⁷⁰ thus, there is an urgent demand for development of effective drugs and vaccines. Several research groups have performed screening studies to identify small molecule inhibitors of arenavirus. Some inhibitors and new compounds have been identified with strong antiarenavirus activity (Table S1); however, the safety profile of these compounds still needs further investigation. In this study, drug repurposing strategy was used, which can significantly reduce the time and resources required to advance a candidate antiviral drug into the clinic setting.⁷¹ These advantages are particularly relevant for the emerging viral diseases, for example, repurposing of remdesivir to treat COVID-19.^{72,73} Several studies have identified drugs with antiarenavirus activity, including tetrandrine and isavuconazole.^{64,74} By comparing with these studies, several hits identified here are with strong antiarenavirus activity (Table S1), among which benidipine hydrochloride was shown to have a strong and broad-spectrum inhibitory effect on arenavirus (Figure 5). In our previous study, benidipine hydrochloride was also found to inhibit severe fever with thrombocytopenia syndrome virus internalization and genome replication.³⁹ The broad-spectrum antiviral effect and general target on the arenavirus fusion structure of benidipine hydrochloride could allow us to better understand the fusion mechanism of arenavirus, while it could also provide a new potential antiviral strategy, as well as arenavirus disease treatment ideas.

As benidipine hydrochloride had previously been reported to have an antiviral effect on SARS-CoV-2,⁷⁵ the antiviral efficacy of the other four drugs, mycophenolic acid, apatinib, dabrafenib, and clofazimine, on SARS-CoV-2 was tested. Of these, mycophenolic acid was found to have the lowest IC₅₀ and a low cell cytotoxicity effect. Mycophenolic acid is an IMPDH inhibitor, and can inhibit guanosine synthesis and cause intracellular GTP depletion. Extra addition of exogenous guanosine to the mycophenolic acid treated cells could restore the intracellular GTP level. Mycophenolic acid was also reported to augment interferon-stimulated gene expression to inhibit hepatitis C virus infection in vitro and in vivo.⁷⁶ Here, we found the antiviral effects of mycophenolic acid on LCMV and SARS-CoV-2 both can be restored by the extra addition of guanosine, suggesting that mycophenolic acid inhibit LCMV and SARS-CoV-2 mainly by depleting intracellular GTP. Our findings reveal that mycophenolic acid is highly effective in the control of LCMV and SARS-CoV-2 infection in vitro (SI > 1000). Since this drug has been used in human patients with a safety track record, it may be applied to human patients under the clinical settings.

METHODS

Cell Lines. BHK-21, Vero, Vero E6, A549, and HEK293T cells were obtained from the American Type Culture Collection (ATCC). BSR-T7 cells, which could stably express the T7 polymerase, were kindly provided by Dr. Mingzhou Chen (Wuhan University, China). BHK-21, Vero, Vero E6, A549, and HEK293T cells were maintained at 37 °C, 5% CO₂, in Dulbecco's modified Eagle medium (DMEM; Gibco), supplemented with 10% fetal bovine serum (FBS, Gibco). BSR-T7 cells were cultured in DMEM with 10% FBS and 1 mg/mL G418 (Merck, CAS #108321-42-2). The mouse spleen cells were separated from fresh mouse spleen, and cultured in RPMI 1640 (Gibco) with 10% FBS.

Reagents. The FDA-approved drug library, mycophenolic acid (chemical abstracts service (CAS) #24280-93-1), clofazimine (CAS #2030-63-9), dabrafenib (CAS #1195765-45-7), apatinib (CAS #811803-05-1), amlodipine (CAS #88150-42-9), benidipine hydrochloride (CAS #91599-74-5), ribavirin (CAS #36791-04-5), remdesivir (CAS #1809249-37-3), cilnidipine (CAS #132203-70-4), clevidipine (CAS #167221-71-8), felodipine (CAS #72509-76-3), nicardipine (CAS #54527-84-3), and nilvadipine (CAS #75530-68-6) were purchased from Selleck Chemicals (Houston, TX, USA). Ammonium chloride (CAS #12125-02-9), BAPTA (CAS #85233-19-8), guanosine (CAS #118-00-3) and Giemsa Stain (CAS #51811-82-6) were purchased from Sigma-Aldrich. Methyl- β -cyclodextrin (CAS #128446-36-6) was purchased from BioLegend. The calcium free DMEM medium (Cat #21068-028, Gibco) was purchased from Gibco. Dimethyl sulfoxide (DMSO) was used as the solvent of these drugs for all cell experiments.

Plasmids. For virus rescue, the LCMV (Armstrong strain 53b) genome RNA L segment (GenBank: AY847351.1) and S segment (GenBank: AY847350.1) were chemically synthesized by Sangon Biotech (Shanghai, China). To obtain the plasmids pT7-L_{LCMV} and pT7-S_{LCMV}, LCMV S and L sequences were cloned and inserted between the T7 polymerase promoter and the hepatitis delta riboenzyme (HDR) sequence in the pT7 vector in an antigenomic direction. The complete LCMV NP, GPC, and L genes were subcloned into the pCAGGS expression vector to generate the plasmids pCAGGS-NP, pCAGGS-GPC, and pCAGGS-L. To construct the LCMV minigenome (MG) reporter gene system, the GPC ORF on the plasmid pT7-S_{LCMV} was replaced by the *Renilla* luciferase gene ORF, and the plasmid pT7-LCMV- Δ GPC/Luc was generated.

Viruses. LCMV was rescued based on a T7 polymerase system described previously.⁷⁷ Viral genome L, genome S, protein NP, and protein L expression plasmids (pT7-L_{LCMV}, pT7-S_{LCMV}, pCAGGS-NP_{LCMV}, and pCAGGS-L_{LCMV}), which are necessary for virus replication and transcription, were cotransfected to the BSR-T7 cells. At 72 h post-transfection, the supernatant containing the generated virus was collected and subsequently amplified in BHK-21 cells.⁷⁸ The eGFP-expressed virus (LCMV-P2A-eGFP) was rescued as previously described.³¹ The recombinant LCMV expressing LASV GPC (LCMV Δ GPC/LASV GPC) was also rescued as previously described.⁷⁹

To obtain the arenavirus GPC- and VSV G-coated pseudotype vesicular stomatitis virus (VSV), HEK293T cells were transfected with arenavirus GPC or VSV G expression plasmids 24 h prior, and the cells were infected with vesicular

stomatitis virus—whose G protein ORF was replaced by the *Renilla luciferase* ORF. The cells were washed and cultured in fresh DMEM with 2% FBS 1 h p.i. For another 24 h, the supernatant containing the pseudotype virus was collected and centrifuged to remove the cell debris, and the arenavirus GPC- or VSV G-coated pseudotype VSV was generated. All virus suspensions were stored at -80°C for further use.

The SARS-CoV-2 used in our experiments is a clinical isolate nCoV-2019BetaCoV/Wuhan/WIV04/2019¹ which propagated in Vero E6 cells. Viral titer of SARS-CoV-2 was determined by 50% tissue culture infective dose (TCID₅₀) using the immunofluorescence assay. All the SARS-CoV-2 infection experiments were performed in biosafety level-3 (BSL-3) laboratory.

Virus Titration. LCMV titer was determined via an immunological plaque assay using antibodies targeting LCMV NP. The virus was 10-fold serially diluted in DMEM, then added to the preseeded BHK-21 cells and incubated at 37°C , 5% CO₂ for 3 h. The supernatant was removed, and 1.1% carboxy methyl cellulose (CMC) in DMEM with 2% FBS was added to the cells. After incubation at 37°C for 72 h, the cells were fixed with 4% formaldehyde and permeabilized by 0.3% Triton X-100 in phosphate-buffered saline (PBS) containing 5% defatted milk powder. Then, the cells were reacted with rabbit polyclonal antibodies to LCMV NP, followed by an antirabbit second antibody, and staining with 3,3'-diaminobenzidine (DAB). The titers were determined by counting the dark-brown plaques on the cells.

Cell Viability. Cells were preseeded on 96-well plates (1.5×10^4 /well) 16 h prior, then treated with a series of dilutions of drugs before incubating at 37°C for 36 h. The cell supernatant was removed, and $50\ \mu\text{L}$ 0.5% 3-(4,5-dimethyl-2-thiazolyl)-2,5-diphenyl-2H-tetrazolium bromide (MTT; Sigma-Aldrich; CAS #298–93–1) dissolved in PBS was added to the cells. In actively growing cells, MTT can utilize reduced nicotinamide adenine dinucleotide (NADH)- and reduced nicotinamide adenine dinucleotide phosphate (NADPH)-dependent cellular oxidoreductase enzymes, producing a blue formazan product that is freely soluble in DMSO.⁸⁰ After incubation at 37°C for 4 h, the supernatant was removed carefully, and $50\ \mu\text{L}$ DMSO was added to the cells. After being gently shaken, the plates were measured at 492 nm using a spectrophotometer, and cell viability was calculated.

LCMV Minigenome Rescue. The minigenome rescue assay was performed as previously described.^{81,82} Briefly, BSR-T7 cells were seeded (1×10^5 /well) on 24-well plates 16 h pretransfection. The plasmids pCAGGS-NP (150 ng), pCAGGS-L (300 ng), pT7-LCMV- Δ GPC/Luc (150 ng), and pRL-TK (50 ng) were transfected to BSR-T7 cells per well using lipo3000 (Invitrogen). Different dilutions of the drugs were added to the cells 4 h post-transfection; then, 48 h later, the cells were lysed and luciferase activity was measured using a luciferase reporter gene assay kit (Beyotime).

Drug Inhibition Effects on LCMV Binding and Internalization. To identify the effect of drugs on LCMV binding, the drugs pretreated with BHK-21 cells were precooled at 4°C for 15 min, then infected with precooled LCMV (MOI = 0.1) at 4°C for 1 h. After that, cells were washed three times with cold PBS; then, cells were lysed and tested by qRT-PCR. To identify the effect of the drugs on LCMV internalization, the drugs pretreated BHK-21 cells were also precooled at 4°C for 15 min, then infected with precooled LCMV (MOI = 0.1) at 4°C for 1 h. After that, the

cells were washed with PBS containing drugs, then transferred to 37°C and incubated for another 3 h. Next, the supernatant was removed, and the cells were digested with 0.25% trypsin for 5 min, then the digestion was terminated by DMEM with 10% FBS. The medium was centrifuged to collect the cells, then the cells were tested by qRT-PCR. Methyl- β -cyclodextrin (M β CD), which is able to remove cell membrane cholesterol to prevent virus internalization, was also used as a positive control.⁸³ Furthermore, in our study, M β CD showed significant inhibition activity on LCMV internalization (Figure 4B).

The Postendosomal Assay. BHK-21 cells were infected with LCMV (MOI = 0.1); simultaneously, to synchronize the virus in the endosome and to avoid membrane fusion, cells were also treated with 20 mM ammonium chloride for 1 h. Then the drugs were added in the presence of ammonium chloride for 30 min, after which the cells were washed to remove ammonium chloride, and virus membrane fusion started. Finally, the cells were incubated with drugs for 16 h altogether and tested by qRT-PCR. To exclude the potential effects of the drugs on replication during the postendosomal assay, a supplementary postentry assay was also developed. The operation procedures were same except being treated with ammonium chloride. BHK-21 cells were infected with LCMV (MOI = 0.1). One hour p.i., drugs were added to cells and cells were incubated at 37°C for 16 h. Then cells were lysed and tested by qRT-PCR.

Quantitative Real-Time PCR (qRT-PCR). The cells were harvested and lysed by TRK lysis buffer (OMEGA biotec, R6834). The clear supernatant was collected after centrifugation. Then, the total RNA of the cells was purified using a total RNA kit (OMEGA biotec, R6834). Purified RNA was dissolved in ribonuclease-free water and stored at -80°C for further use. The residual genome DNA in the total RNA was removed using deoxyribonuclease, and the total RNA was reverse transcribed into cDNA using a PrimeScript RT reagent kit (Takara, RR047A). Viral genome RNA in the supernatant was extracted by viral DNA/RNA extraction kit (Takara, 9766), and was also reverse transcribed into cDNA by PrimeScript RT reagent kit. The LCMV NP fragment was quantified with primers 5'-GTACAAGCGCTCACAGACCT-3' and 5'-GTTACCCCATCCAACAGGG-3'; the SARS-CoV-2 genome was quantified with primers 5'-CAATG-GTTTAAACAGGCACAGG-3' and 5'-CTCAAGTGTC-TGTGGATCACG-3'; the Vero cells' GAPDH fragment was quantified with primers 5'-GGTGGTCCTCTGACT-TCAACA-3' and 5'-GTTGCTGTAGCCAAATTCGTTGT-3'; the BHK-21 cells' GAPDH fragment was quantified with primers 5'-ATCCCACCAACATCAAATGG-3' and 5'-AAGACGCCAGTAGACTCCACA-3'; the A549 cells' GAPDH fragment was quantified with primers 5'-GAAGG-TGAAGTTCGGAGTC-3' and 5'-GAAGATGGTGATGGG-ATTTTC-3'; and the mouse spleen cells' tubulin fragment was quantified with primers 5'-TGCCTTTGTGCACTGGTATG-3' and 5'-CTGGAGCAGTTTGACGACAC-3'.

Immunofluorescence Assay (IFA). The drugs treated Vero E6 cells were infected with SARS-CoV-2 and the supernatant was collected 24 h p.i. to test the antiviral efficacy of drugs. After the supernatant was collected, the SARS-CoV-2 infected cells were fixed with 4% formaldehyde for at least 1h at room temperature. Then the fixed cells were permeabilized by 0.3% Triton X-100 in PBS and blocked by 5% FBS in PBS at room temperature for 1 h. After washed with PBS for three

times, cells were probed with the primary antibody, a polyclonal antibody against viral nucleocapsid protein of a bat SARS-related coronavirus,⁸⁴ for 2 h at room temperature. After being washed with PBS for five times, cells were probed with the secondary antibody Alexa 488-labeled goat antirabbit IgG (1:300; Abcam) for 1 h. The nuclei were stained with DAPI (Sigma, CAS # 28718–90–3), after being washed five times, and images were captured under a fluorescent microscopy (Nikon A1MP STORM).

■ ASSOCIATED CONTENT

Supporting Information

The Supporting Information is available free of charge at <https://pubs.acs.org/doi/10.1021/acsinfecdis.0c00486>.

Figure S1: The antiviral effects of the positive control drugs; Figure S2: Dose-dependent anti-LCMV effects of mycophenolic acid, clofazimine, apatinib, benidipine hydrochloride, and dabrafenib on A549 cells; Figure S3: Antiviral effects of the five drugs on mouse spleen cells; Figure S4: Antiviral effect of benidipine hydrochloride on arenaviruses GPC mediated entry process; Figure S5: Comparison of the entry kinetics between wild type and the GPC D414A mutant LCMV; Figure S6: The effect of calcium on LCMV replication; Table S1: Activities of small molecule inhibitors against arenavirus multiplication (PDF)

■ AUTHOR INFORMATION

Corresponding Authors

Gengfu Xiao – State Key Laboratory of Virology, Wuhan Institute of Virology, Chinese Academy of Sciences, Wuhan, Hubei 430071, PR China; University of Chinese Academy of Sciences, Beijing 100049, PR China; Email: xiaogf@wh.iov.cn

Ke Peng – State Key Laboratory of Virology, Wuhan Institute of Virology, Chinese Academy of Sciences, Wuhan, Hubei 430071, PR China; University of Chinese Academy of Sciences, Beijing 100049, PR China; Email: pengke@wh.iov.cn

Leike Zhang – State Key Laboratory of Virology, Wuhan Institute of Virology, Chinese Academy of Sciences, Wuhan, Hubei 430071, PR China; University of Chinese Academy of Sciences, Beijing 100049, PR China; orcid.org/0000-0002-2593-2571; Email: zhangleike@wh.iov.cn

Authors

Weiwei Wan – State Key Laboratory of Virology, Wuhan Institute of Virology, Chinese Academy of Sciences, Wuhan, Hubei 430071, PR China; University of Chinese Academy of Sciences, Beijing 100049, PR China

Shenglin Zhu – State Key Laboratory of Virology, Wuhan Institute of Virology, Chinese Academy of Sciences, Wuhan, Hubei 430071, PR China

Shufen Li – State Key Laboratory of Virology, Wuhan Institute of Virology, Chinese Academy of Sciences, Wuhan, Hubei 430071, PR China

Weijuan Shang – State Key Laboratory of Virology, Wuhan Institute of Virology, Chinese Academy of Sciences, Wuhan, Hubei 430071, PR China

Ruxue Zhang – State Key Laboratory of Virology, Wuhan Institute of Virology, Chinese Academy of Sciences, Wuhan, Hubei 430071, PR China

Hao Li – Beijing Institute of Microbiology and Epidemiology, State Key Laboratory of Pathogen and Biosecurity, Beijing 100071, PR China

Wei Liu – Beijing Institute of Microbiology and Epidemiology, State Key Laboratory of Pathogen and Biosecurity, Beijing 100071, PR China

Complete contact information is available at: <https://pubs.acs.org/doi/10.1021/acsinfecdis.0c00486>

Notes

The authors declare no competing financial interest.

■ ACKNOWLEDGMENTS

We thank Hao Tang, Jia Wu, Jun Liu, and Tao Du from BSL-3 Laboratory of Wuhan Institute of Virology for their critical support. We thank Xuefang An, Ding Gao in the Core Facility and Technical Support Facility of the Wuhan Institute of Virology for their technical assistance. The study was supported by the National Science and Technology Major Project (2018ZX10101004001005), the Natural Science Foundation of China (31970165, 81825019, 81722041, 31770188), the Open Research Fund Program of Wuhan National Bio-Safety Level 4 Lab of CAS (2018ACCP-MS01, 2020ACCP-MS02), the Hubei Science and Technology Project (2020FCA003), and the Youth Innovation Promotion Association CAS (grants 2018367 to L.-K.Z.).

■ REFERENCES

- (1) Pinschewer, D. D., Perez, M., and de la Torre, J. C. (2005) Dual role of the lymphocytic choriomeningitis virus intergenic region in transcription termination and virus propagation. *J. Virol.* 79, 4519–4526.
- (2) Buchmeier, M., Peters, C. J., and De la Torre, J. C. (2007) Arenaviridae: the viruses and their replication. In *Fields Virology*, 5th ed. (Knipe, D., Howley, P. M., Griffin, D. E., Lamb, R. A., Martin, M. A., Roizman, B., and Straus, S. E., Eds.) pp 1791–1828, Lippincott Williams & Wilkins, Philadelphia, PA.
- (3) Emonet, S. E., Urata, S., and de la Torre, J. C. (2011) Arenavirus reverse genetics: new approaches for the investigation of arenavirus biology and development of antiviral strategies. *Virology* 411, 416–425.
- (4) Riviere, Y., Ahmed, R., Southern, P. J., Buchmeier, M. J., Dutko, F. J., and Oldstone, M. B. (1985) The S RNA segment of lymphocytic choriomeningitis virus codes for the nucleoprotein and glycoproteins 1 and 2. *J. Virol.* 53, 966–968.
- (5) Beyer, W. R., Popplau, D., Garten, W., von Laer, D., and Lenz, O. (2003) Endoproteolytic Processing of the Lymphocytic Choriomeningitis Virus Glycoprotein by the Subtilase SKI-1/S1P. *J. Virol.* 77, 2866–2872.
- (6) Wright, K. E., Spiro, R. C., Burns, J. W., and Buchmeier, M. J. (1990) Post-translational processing of the glycoproteins of lymphocytic choriomeningitis virus. *Virology* 177, 175–183.
- (7) Agnihothram, S. S., York, J., Trahey, M., and Nunberg, J. H. (2007) Bitopic membrane topology of the stable signal peptide in the tripartite Junin virus GP-C envelope glycoprotein complex. *J. Virol.* 81, 4331–4337.
- (8) York, J., and Nunberg, J. H. (2006) Role of the stable signal peptide of Junin arenavirus envelope glycoprotein in pH-dependent membrane fusion. *J. Virol.* 80, 7775–7780.
- (9) Eichler, R., Lenz, O., Strecker, T., Eickmann, M., Klenk, H. D., and Garten, W. (2003) Identification of Lassa virus glycoprotein signal peptide as a trans-acting maturation factor. *EMBO Rep.* 4, 1084–1088.
- (10) Burri, D. J., Pasquato, A., da Palma, J. R., Igonet, S., Oldstone, M. B., and Kunz, S. (2013) The role of proteolytic processing and the

stable signal peptide in expression of the Old World arenavirus envelope glycoprotein ectodomain. *Virology* 436, 127–133.

(11) York, J., Romanowski, V., Lu, M., and Nunberg, J. H. (2004) The signal peptide of the Junin arenavirus envelope glycoprotein is myristoylated and forms an essential subunit of the mature G1-G2 complex. *J. Virol.* 78, 10783–10792.

(12) Radoshitzky, S. R., Bao, Y., Buchmeier, M. J., Charrel, R. N., Clawson, A. N., Clegg, C. S., DeRisi, J. L., Emonet, S., Gonzalez, J. P., Kuhn, J. H., Lukashevich, I. S., Peters, C. J., Romanowski, V., Salvato, M. S., Stenglein, M. D., and de la Torre, J. C. (2015) Past, present, and future of arenavirus taxonomy. *Arch. Virol.* 160, 1851–1874.

(13) Peters, C. J. (2002) Human infection with arenaviruses in the Americas. *Curr. Top. Microbiol. Immunol.* 262, 65–74.

(14) Grande-Perez, A., Martin, V., Moreno, H., and de la Torre, J. C. (2015) Arenavirus Quasispecies and Their Biological Implications. *Curr. Top. Microbiol. Immunol.* 392, 231–275.

(15) McCormick, J. B., Webb, P. A., Krebs, J. W., Johnson, K. M., and Smith, E. S. (1987) A prospective study of the epidemiology and ecology of Lassa fever. *J. Infect. Dis.* 155, 437–444.

(16) Enria, D. A., Briggiler, A. M., and Sanchez, Z. (2008) Treatment of Argentine hemorrhagic fever. *Antiviral Res.* 78, 132–139.

(17) Parker, J. C., Igel, H. J., Reynolds, R. K., Lewis, A. M., Jr, and Rowe, W. P. (1976) Lymphocytic choriomeningitis virus infection in fetal, newborn, and young adult Syrian hamsters (*Mesocricetus auratus*). *Infect. Immun.* 13, 967–981.

(18) Mets, M. B., Barton, L. L., Khan, A. S., and Ksiazek, T. G. (2000) Lymphocytic choriomeningitis virus: an underdiagnosed cause of congenital chorioretinitis. *Am. J. Ophthalmol.* 130, 209–215.

(19) Peters, C. J. (2006) Lymphocytic choriomeningitis virus—an old enemy up to new tricks. *N. Engl. J. Med.* 354, 2208–2211.

(20) Barton, L. L., and Hyndman, N. J. (2000) Lymphocytic choriomeningitis virus: reemerging central nervous system pathogen. *Pediatrics* 105, E35.

(21) Barton, L. L., Mets, M. B., and Beauchamp, C. L. (2002) Lymphocytic choriomeningitis virus: emerging fetal teratogen. *Am. J. Obstet. Gynecol.* 187, 1715–1716.

(22) Fischer, S. A., Graham, M. B., Kuehnert, M. J., Kotton, C. N., Srinivasan, A., Marty, F. M., Comer, J. A., Guarner, J., Paddock, C. D., DeMeo, D. L., Shieh, W. J., Erickson, B. R., Bandy, U., DeMaria, A., Jr, Davis, J. P., Delmonico, F. L., Pavlin, B., Likos, A., Vincent, M. J., Sealy, T. K., Goldsmith, C. S., Jernigan, D. B., Rollin, P. E., Packard, M. M., Patel, M., Rowland, C., Helfand, R. F., Nichol, S. T., Fishman, J. A., Ksiazek, T., and Zaki, S. R. (2006) Transmission of lymphocytic choriomeningitis virus by organ transplantation. *N. Engl. J. Med.* 354, 2235–2249.

(23) Centers for Disease Control and Prevention. (2005) Lymphocytic choriomeningitis virus infection in organ transplant recipients—Massachusetts, Rhode Island, 2005. In *MMWR Morbidity and Mortality Weekly Report*, Vol. 54, pp 537–539.

(24) Bonthius, D. J., Nichols, B., Harb, H., Mahoney, J., and Karacay, B. (2007) Lymphocytic choriomeningitis virus infection of the developing brain: critical role of host age. *Ann. Neurol.* 62, 356–374.

(25) Bonthius, D. J., and Perlman, S. (2007) Congenital viral infections of the brain: lessons learned from lymphocytic choriomeningitis virus in the neonatal rat. *PLoS Pathog.* 3, No. e149.

(26) Kilgore, P. E., Peters, C. J., Mills, J. N., Rollin, P. E., Armstrong, L., Khan, A. S., and Ksiazek, T. G. (1995) Prospects for the control of Bolivian hemorrhagic fever. *Emerging Infect. Dis.* 1, 97–100.

(27) Kilgore, P. E., Ksiazek, T. G., Rollin, P. E., Mills, J. N., Villagra, M. R., Montenegro, M. J., Costales, M. A., Paredes, L. C., and Peters, C. J. (1997) Treatment of Bolivian hemorrhagic fever with intravenous ribavirin. *Clin. Infect. Dis.* 24, 718–722.

(28) Huggins, J. W. (1989) Prospects for treatment of viral hemorrhagic fevers with ribavirin, a broad-spectrum antiviral drug. *Clin. Infect. Dis.* 11 (4), S750–S761.

(29) McCormick, J. B., King, I. J., Webb, P. A., Scribner, C. L., Craven, R. B., Johnson, K. M., Elliott, L. H., and Belmont-Williams, R.

(1986) Lassa fever. Effective therapy with ribavirin. *N. Engl. J. Med.* 314, 20–26.

(30) World Health Organization. (2020) *Coronavirus Disease (COVID-19) Weekly Epidemiological Update and Weekly Operational Update—23 October 2020*.

(31) Ngo, N., Cubitt, B., Iwasaki, M., and de la Torre, J. C. (2015) Identification and Mechanism of Action of a Novel Small-Molecule Inhibitor of Arenavirus Multiplication. *J. Virol.* 89, 10924–10933.

(32) Zhang, J. H., Chung, T. D., and Oldenburg, K. R. (1999) A Simple Statistical Parameter for Use in Evaluation and Validation of High Throughput Screening Assays. *J. Biomol. Screening* 4, 67–73.

(33) Iwasaki, M., Ngo, N., and de la Torre, J. C. (2014) Sodium hydrogen exchangers contribute to arenavirus cell entry. *J. Virol.* 88, 643–654.

(34) Opplinger, J., Torriani, G., Herrador, A., and Kunz, S. (2016) Lassa Virus Cell Entry via Dystroglycan Involves an Unusual Pathway of Macropinocytosis. *J. Virol.* 90, 6412–6429.

(35) Banerjee, I., Miyake, Y., Nobs, S. P., Schneider, C., Horvath, P., Kopf, M., Matthias, P., Helenius, A., and Yamauchi, Y. (2014) Influenza A virus uses the aggresome processing machinery for host cell entry. *Science* 346, 473–437.

(36) Kosaka, H., Hirayama, K., Yoda, N., Sasaki, K., Kitayama, T., Kusaka, H., and Matsubara, M. (2010) The L-, N-, and T-type triple calcium channel blocker benidipine acts as an antagonist of mineralocorticoid receptor, a member of nuclear receptor family. *Eur. J. Pharmacol.* 635, 49–55.

(37) Yamamoto, M., Gotoh, Y., Imaizumi, Y., and Watanabe, M. (1990) Mechanisms of long-lasting effects of benidipine on Ca current in guinea-pig ventricular cells. *Br. J. Pharmacol.* 100, 669–676.

(38) Matsubara, M., and Hasegawa, K. (2005) Benidipine, a dihydropyridine-calcium channel blocker, prevents lysophosphatidylcholine-induced injury and reactive oxygen species production in human aortic endothelial cells. *Atherosclerosis* 178, 57–66.

(39) Li, H., Zhang, L. K., Li, S. F., Zhang, S. F., Wan, W. W., Zhang, Y. L., Xin, Q. L., Dai, K., Hu, Y. Y., Wang, Z. B., Zhu, X. T., Fang, Y. J., Cui, N., Zhang, P. H., Yuan, C., Lu, Q. B., Bai, J. Y., Deng, F., Xiao, G. F., Liu, W., and Peng, K. (2019) Calcium channel blockers reduce severe fever with thrombocytopenia syndrome virus (SFTSV) related fatality. *Cell Res.* 29, 739–753.

(40) Olschlager, S., Neyts, J., and Gunther, S. (2011) Depletion of GTP pool is not the predominant mechanism by which ribavirin exerts its antiviral effect on Lassa virus. *Antiviral Res.* 91, 89–93.

(41) Diamond, M. S., Zachariah, M., and Harris, E. (2002) Mycophenolic Acid Inhibits Dengue Virus Infection by Preventing Replication of Viral RNA. *Virology* 304, 211–221.

(42) Padalko, E., Verbeke, E., Matthyss, P., Aerts, J. L., De Clercq, E., and Neyts, J. (2003) Mycophenolate mofetil inhibits the development of Coxsackie B3-virus-induced myocarditis in mice. *BMC Microbiol.* 3, 25.

(43) Henry, S. D., Metselaar, H. J., Lonsdale, R. C., Kok, A., Haagmans, B. L., Tilanus, H. W., and van der Laan, L. J. (2006) Mycophenolic acid inhibits hepatitis C virus replication and acts in synergy with cyclosporin A and interferon-alpha. *Gastroenterology* 131, 1452–1462.

(44) Wang, Y., Zhou, X., Debing, Y., Chen, K., Van Der Laan, L. J., Neyts, J., Janssen, H. L., Metselaar, H. J., Peppelenbosch, M. P., and Pan, Q. (2014) Calcineurin inhibitors stimulate and mycophenolic acid inhibits replication of hepatitis E virus. *Gastroenterology* 146, 1775–1783.

(45) Yao, K., Nagashima, K., and Miki, H. (2006) Pharmacological, pharmacokinetic, and clinical properties of benidipine hydrochloride, a novel, long-acting calcium channel blocker. *J. Pharmacol. Sci.* 100, 243–261.

(46) Ishii, A., Nishida, K., Oka, T., and Nakamizo, N. (1988) Receptor binding properties of the new calcium antagonist benidipine hydrochloride. *Arzneimittelforschung* 38, 1677–1680.

(47) Ishii, A., Nishida, K., Oka, T., and Nakamizo, N. (1988) Slow dissociation of the new slow-onset and long-acting calcium antagonist

benidipine hydrochloride from 3H-nitrendipine binding sites. *Arzneimittelforschung* 38, 1681–1683.

(48) Masumoto, K., Takeyasu, A., Oizumi, K., and Kobayashi, T. (1995) [Studies of novel 1,4-dihydropyridine Ca antagonist CS-905. I. Measurement of partition coefficient (log P) by high performance liquid chromatography (HPLC)]. *Yakugaku Zasshi* 115, 213–220.

(49) Rhodes, D. G., Sarmiento, J. G., and Herbet, L. G. (1985) Kinetics of binding of membrane-active drugs to receptor sites. Diffusion-limited rates for a membrane bilayer approach of 1,4-dihydropyridine calcium channel antagonists to their active site. *Mol. Pharmacol.* 27, 612–623.

(50) Karasawa, A., and Kubo, K. (1990) Protection by benidipine hydrochloride (KW-3049), a calcium antagonist, of ischemic kidney in rats via inhibitions of Ca-overload, ATP-decline and lipid peroxidation. *Jpn. J. Pharmacol.* 52, 553–562.

(51) Yao, K., Sato, H., Ina, Y., Nagashima, K., Nishikawa, S., Ohmori, K., and Ohno, T. (2000) Benidipine inhibits apoptosis during ischaemic acute renal failure in rats. *J. Pharm. Pharmacol.* 52, 561–568.

(52) Yao, K., and Karasawa, A. (1994) Protective effects of benidipine against myocardial damage following ischemia and reperfusion in the isolated perfused rat heart. *Biol. Pharm. Bull.* 17, 517–521.

(53) Kitakaze, M., Karasawa, A., Kobayashi, H., Tanaka, H., Kuzuya, T., and Hori, M. (1999) Benidipine: a new Ca²⁺ channel blocker with a cardioprotective effect. *Cardiovasc. Drug Rev.* 17 (1), 1–15.

(54) Moreno, H., Gallego, I., Sevilla, N., de la Torre, J. C., Domingo, E., and Martin, V. (2011) Ribavirin can be mutagenic for arenaviruses. *J. Virol* 85, 7246–7255.

(55) Cao, W., Henry, M. D., Borrow, P., Yamada, H., Elder, J. H., Ravkov, E. V., Nichol, S. T., Compans, R. W., Campbell, K. P., and Oldstone, M. B. (1998) Identification of alpha-dystroglycan as a receptor for lymphocytic choriomeningitis virus and Lassa fever virus. *Science* 282, 2079–2081.

(56) Smelt, S. C., Borrow, P., Kunz, S., Cao, W., Tishon, A., Lewicki, H., Campbell, K. P., and Oldstone, M. B. (2001) Differences in affinity of binding of lymphocytic choriomeningitis virus strains to the cellular receptor alpha-dystroglycan correlate with viral tropism and disease kinetics. *J. Virol.* 75, 448–457.

(57) Radoshitzky, S. R., Abraham, J., Spiropoulou, C. F., Kuhn, J. H., Nguyen, D., Li, W., Nagel, J., Schmidt, P. J., Nunberg, J. H., Andrews, N. C., Farzan, M., and Choe, H. (2007) Transferrin receptor 1 is a cellular receptor for New World haemorrhagic fever arenaviruses. *Nature* 446, 92–96.

(58) Kim, I. S., Jenni, S., Stanifer, M. L., Roth, E., Whelan, S. P., van Oijen, A. M., and Harrison, S. C. (2017) Mechanism of membrane fusion induced by vesicular stomatitis virus G protein. *Proc. Natl. Acad. Sci. U. S. A.* 114, E28–E36.

(59) York, J., and Nunberg, J. H. (2009) Intersubunit interactions modulate pH-induced activation of membrane fusion by the Junin virus envelope glycoprotein GPC. *J. Virol.* 83, 4121–4126.

(60) Shankar, S., Whitby, L. R., Casquilho-Gray, H. E., York, J., Boger, D. L., and Nunberg, J. H. (2016) Small-molecule fusion inhibitors bind the pH-sensing SSP-GP2 subunit interface of the Lassa virus envelope glycoprotein. *J. Virol.* 90, 6799–6807.

(61) Larson, R. A., Dai, D., Hosack, V. T., Tan, Y., Bolken, T. C., Hruby, D. E., and Amberg, S. M. (2008) Identification of a broad-spectrum arenavirus entry inhibitor. *J. Virol.* 82, 10768–10775.

(62) York, J., Dai, D., Amberg, S. M., and Nunberg, J. H. (2008) pH-induced activation of arenavirus membrane fusion is antagonized by small-molecule inhibitors. *J. Virol.* 82, 10932–10939.

(63) Lavanya, M., Cuevas, C. D., Thomas, M., Cherry, S., and Ross, S. R. (2013) siRNA screen for genes that affect Junin virus entry uncovers voltage-gated calcium channels as a therapeutic target. *Sci. Transl. Med.* 5, 204ra131.

(64) Rathbun, J. Y., Droniou, M. E., Damoiseaux, R., Haworth, K. G., Henley, J. E., Exline, C. M., Choe, H., and Cannon, P. M. (2015) Novel Arenavirus Entry Inhibitors Discovered by Using a

Minigenome Rescue System for High-Throughput Drug Screening. *J. Virol.* 89, 8428–8443.

(65) Wang, P., Liu, Y., Zhang, G., Wang, S., Guo, J., Cao, J., Jia, X., Zhang, L., Xiao, G., and Wang, W. (2018) Screening and Identification of Lassa Virus Entry Inhibitors from an FDA-Approved Drug Library. *J. Virol.* 92, 92.

(66) Sarute, N., and Ross, S. R. (2020) CACNA1S haploinsufficiency confers resistance to New World arenavirus infection. *Proc. Natl. Acad. Sci. U. S. A.* 117, 19497–19506.

(67) Gehring, G., Rohrmann, K., Atenchong, N., Mittler, E., Becker, S., Dahlmann, F., Pohlmann, S., Vondran, F. W., David, S., Manns, M. P., Ciesek, S., and von Hahn, T. (2014) The clinically approved drugs amiodarone, dronedarone and verapamil inhibit filovirus cell entry. *J. Antimicrob. Chemother.* 69, 2123–2131.

(68) Fujioka, Y., Nishide, S., Ose, T., Suzuki, T., Kato, I., Fukuhara, H., Fujioka, M., Horiuchi, K., Satoh, A. O., Nepal, P., Kashiwagi, S., Wang, J., Horiguchi, M., Sato, Y., Paudel, S., Nanbo, A., Miyazaki, T., Hasegawa, H., Maenaka, K., and Ohba, Y. (2018) A Sialylated Voltage-Dependent Ca(2+) Channel Binds Hemagglutinin and Mediates Influenza A Virus Entry into Mammalian Cells. *Cell Host Microbe* 23, 809–818.

(69) Sakurai, Y., Kolokoltsov, A. A., Chen, C. C., Tidwell, M. W., Bauta, W. E., Klugbauer, N., Grimm, C., Wahl-Schott, C., Biel, M., and Davey, R. A. (2015) Ebola virus. Two-pore channels control Ebola virus host cell entry and are drug targets for disease treatment. *Science* 347, 995–958.

(70) Geisbert, T. W., and Jahrling, P. B. (2004) Exotic emerging viral diseases: progress and challenges. *Nat. Med.* 10, S110–S121.

(71) Kim, S., Chen, J., Cheng, T., Gindulyte, A., He, J., He, S., Li, Q., Shoemaker, B. A., Thiessen, P. A., Yu, B., Zaslavsky, L., Zhang, J., and Bolton, E. E. (2019) PubChem. 2019 update: improved access to chemical data. *Nucleic Acids Res.* 47, D1102–D1109.

(72) Wang, M., Cao, R., Zhang, L., Yang, X., Liu, J., Xu, M., Shi, Z., Hu, Z., Zhong, W., and Xiao, G. (2020) Remdesivir and chloroquine effectively inhibit the recently emerged novel coronavirus (2019-nCoV) in vitro. *Cell Res.* 30, 269–271.

(73) Beigel, J. H., Tomashek, K. M., Dodd, L. E., Mehta, A. K., Zingman, B. S., Kalil, A. C., Hohmann, E., Chu, H. Y., Luetkemeyer, A., Kline, S., Lopez de Castilla, D., Finberg, R. W., Dierberg, K., Tanson, V., Hsieh, L., Patterson, T. F., Paredes, R., Sweeney, D. A., Short, W. R., Touloumi, G., Lye, D. C., Ohmagari, N., Oh, M.-d., Ruiz-Palacios, G. M., Benfield, T., Fatkenheuer, G., Kortepeter, M. G., Atmar, R. L., Creech, C. B., Lundgren, J., Babiker, A. G., Pett, S., Neaton, J. D., Burgess, T. H., Bonnett, T., Green, M., Makowski, M., Osinusi, A., Nayak, S., and Lane, H. C. (2020) Remdesivir for the Treatment of Covid-19 - Final Report. *N. Engl. J. Med.* 383, 1813.

(74) Zhang, X., Tang, K., and Guo, Y. (2020) The antifungal isavuconazole inhibits the entry of lassa virus by targeting the stable signal peptide-GP2 subunit interface of lassa virus glycoprotein. *Antiviral Res.* 174, 104701.

(75) Zhang, L., Sun, Y., Zeng, H.-L., Peng, Y., Jiang, X., Shang, W.-J., Wu, Y., Li, S., Zhang, Y.-L., and Yang, L. (2020) Calcium channel blocker amlodipine besylate is associated with reduced case fatality rate of COVID-19 patients with hypertension. *medRxiv*, Apr 14, 2020, DOI: 10.1101/2020.04.08.20047134 (accessed 2020-10-10).

(76) Pan, Q., de Ruiter, P. E., Metselaar, H. J., Kwekkeboom, J., de Jonge, J., Tilanus, H. W., Janssen, H. L., and van der Laan, L. J. (2012) Mycophenolic acid augments interferon-stimulated gene expression and inhibits hepatitis C Virus infection in vitro and in vivo. *Hepatology* 55, 1673–1683.

(77) Sanchez, A. B., and de la Torre, J. C. (2006) Rescue of the prototypic Arenavirus LCMV entirely from plasmid. *Virology* 350, 370–380.

(78) Lee, K. J., Novella, I. S., Teng, M. N., Oldstone, M. B., and de La Torre, J. C. (2000) NP and L proteins of lymphocytic choriomeningitis virus (LCMV) are sufficient for efficient transcription and replication of LCMV genomic RNA analogs. *J. Virol.* 74, 3470–3407.

(79) Sommerstein, R., Ramos da Palma, J., Olschlager, S., Bergthaler, A., Barba, L., Lee, B. P., Pasquato, A., and Flatz, L. (2014) Evolution of recombinant lymphocytic choriomeningitis virus/Lassa virus in vivo highlights the importance of the GPC cytosolic tail in viral fitness. *J. Virol.* 88, 8340–8348.

(80) Berridge, M. V., and Tan, A. S. (1993) Characterization of the cellular reduction of 3-(4,5-dimethylthiazol-2-yl)-2,5-diphenyltetrazolium bromide (MTT): subcellular localization, substrate dependence, and involvement of mitochondrial electron transport in MTT reduction. *Arch. Biochem. Biophys.* 303, 474–482.

(81) Hass, M., Golnitz, U., Muller, S., Becker-Ziaja, B., and Gunther, S. (2004) Replicon system for Lassa virus. *J. Virol.* 78, 13793–13803.

(82) de la Torre, J. C. (2008) Reverse genetics approaches to combat pathogenic arenaviruses. *Antiviral Res.* 80, 239–250.

(83) Vela, E. M., Zhang, L., Colpitts, T. M., Davey, R. A., and Aronson, J. F. (2007) Arenavirus entry occurs through a cholesterol-dependent, non-caveolar, clathrin-mediated endocytic mechanism. *Virology* 369, 1–11.

(84) Zhou, P., Yang, X.-L., Wang, X.-G., Hu, B., Zhang, L., Zhang, W., Si, H.-R., Zhu, Y., Li, B., and Huang, C.-L. (2020) Discovery of a novel coronavirus associated with the recent pneumonia outbreak in humans and its potential bat origin. *bioRxiv*, Jan 23, 2020, DOI: 10.1101/2020.01.22.914952 (accessed 2020-10-10).